Available online at www.sciencedirect.com
ScienceDirect
International Journal of Heat and Mass Transfer 50 (2007) 2936–2943
International Journal of HEAT and MASS TRANSFER
www.elsevier.com/locate/ijhmt

Non-thermal equilibrium model of the coupled heat and mass transfer in strong endothermic chemical reaction system of porous media

Mingchun Li [a,*], Yusheng Wu [a], Yanwen Tian [b], Yuchun Zhai [b]

[a] School of Material Science and Engineering, Shenyang University of Technology, Shenyang 110023, China
[b] Institute of Metallurgy Physical Chemistry, Northeastern University, Shenyang 110004, China

Received 15 November 2005; received in revised form 15 December 2006
Available online 1 March 2007

Abstract

A two dimension mathematical model has been developed to simulate the coupled heat and mass transfer in a porous medium undergoing a strong endothermic chemical reaction. Differing from the traditional two phase equation model, just the temperature field of bulk flow is known from the solution of energy equation. The temperature distribution of the solid matrix is solved according to the reaction kinetics of the decomposition of calcium carbonate. The coupling of these two equations is given by the item of chemical reaction. The fluid flow is modeled by the Ergun–Forchheimer–Brinkman equation. This model is solved numerically by the alternate dimension implicit method, and the numerical results are validated by comparing with the experimental data in literature. The influence of the strongly endothermic chemical reaction on the heat and mass transfers in the porous medium is discussed. The reaction features of the packed bed of pellets are analyzed under different conditions by varying the key parameters.

1. Introduction

Flow and heat transfer in porous media have broad applications in nature and engineering practice such as geothermal systems, energy storage units, thermal insulation, packed bed heat exchangers, drying technology, catalytic reactors, and nuclear waste repository. In general, various analytical studies used in dealing with transport processes in porous media hypothesize the existence of local thermal equilibrium [1–4]. But, the utilization of the assumption of local thermal equilibrium breaks down often in many practical applications. Quintard and Whitaker [5] cited numerous physical situations where local thermal equilibrium fails. For example, when there is a significant heat generation occurring in any one of the two phases (solid or fluid), the temperatures in the two phases are no longer identical. When the temperature at the bounding surface changes significantly with respect to time, and when solid and fluid phases have significantly different heat capacities and thermal conductivities, the local rate of change of temperature for one phase differs significantly from that for the other phase. Amiri and Vafai [6] investigated the validity of local thermal equilibrium conditions for steady state as well as transient incompressible flow through a porous medium. Kim et al. [7] presented an analytical solution for two-equation model including the boundary effect for an equivalent microchannel application. They presented analytical solutions for the fluid and solid phase temperature distributions based on the Brinkman-extended Darcy equation. They also analyzed the validity of the local thermal equilibrium assumption.

In the absence of local thermal equilibrium, the single energy equation needs to be replaced with two energy equations, one for the solid and another for the fluid. The coupling of these two equations is given by the interfacial heat transfer coefficient. Two energy equation models have been introduced heuristically in the literature [8]. In recent years, the local thermal non-equilibrium model has been given considerable attention and been utilized in various fields [9] due to its pertinence in applications. For example, Lee

* Corresponding author. Tel.: +86 (0)136 04187687.
E-mail address: liming-799@163.com (M. Li).

0017-9310/$ - see front matter © 2007 Elsevier Ltd. All rights reserved.
doi:10.1016/j.ijheatmasstransfer.2006.12.013

Nomenclature

C^*	molar fraction of species CO_2
C_{CO_2}	concentration of product gas CO_2 (mol m^{-3})
C_p	specific heat of mixture gas (KJ mol^{-1} K^{-1})
C_{p,CO_2}	specific heat of CO_2 (KJ mol^{-1} K^{-1})
$C_{p,d}$	specific heat of inertial gas (KJ mol^{-1} K^{-1})
d	particle diameter (m)
D	effective diffusivity (m^2 s^{-1})
G_A	moles of calcium carbonate (mol)
h_i	interfacial convective heat transfer coefficient (W m^{-2} K^{-1})
ΔH	enthalpy of dissociation (KJ mol^{-1})
k_f	fluid conductivity (W m^{-1} K^{-1})
L	reactor length (m)
M_s	molar mass of calcium carbonate (g/mol)
q_s, q_d, q_r	heat transfer rate (W)
q_w	constant heat flux at the wall (W)
r	coordinate variable in radial direction (m)
r_c	un-reacted core radius, (m)
r_{in}	initial pellet radius, (m)
$\bar{r}$	dimensionless radial coordinate, r/R
R	cylindrical reactor diameter (m)
R_A	overall reaction rate of a single particle (mol s^{-1})
R_V	overall reaction rate on the scale of REV (mol m^{-3} s^{-1})
S_V	specific surface area (m^{-1})
t	time (s)
$\bar{t}$	dimensionless time scale, $\bar{t} = tD/L^2$
T_b	temperature of main stream flows in pore (K)
T_c	unburnt core temperature (K)
T_{in}	initial thermal gas temperature (K)
T_s	surface temperature of the particle (K)
v	effective velocity of fluid flow in porous media (m s^{-1})
v_b	superficial velocity of fluid (m s^{-1})
x	longitudinal coordinate (m)
$\bar{x}$	dimensionless axial length scale, x/L

Greek symbols

λ_e	thermal conductivity of the solid product (W m^{-1} K^{-1})
μ	dynamic viscosity (kg s^{-1} m^{-1})
ε	porosity
ρ	molar density of the mixture gas (mol m^{-3})
ρ_s	limestone density (kg m^{-3})
ρ_f	fluid density (kg m^{-3})

Subscripts/superscripts

f	fluid phase
p	specific heat at constant pressure
s	solid phase/surface
$*$	non-dimensional

and Vafai [10] employed the non-thermal equilibrium model to investigate the forced convective flow through a channel filled with a porous medium. They obtained analytical solutions for the fluid and solid phase temperature distributions. Kuznetsov [11] obtained an interesting perturbation solution for the temperature difference between the solid and liquid phases for the problem of thermal non-equilibrium in a parallel plate channel with constant heat flux using a perturbation approach. However, his analysis could not produce a temperature distribution for any of the phases. Marafie and Vafai [12] obtained analytical expressions for the fluid and solid phase temperature distributions for convective flow through the channel with a constant heat flux applied at walls and accounting for both boundary and inertial effects. By far, most researches related the heat and mass transport in porous media usually focus on the transport processes within an inert porous medium [13–16]. Veldsink et al. [17] adopted the Fick model and the dusty-gas model to study the mass transport accompanied by chemical reaction in porous catalyst. Jaguste and Bhatla [18] investigated simultaneous heat, mass and momentum transport phenomena accompanying phase transition and exothermic chemical reaction in unsaturated capillary porous media with respect to a partially externally wetted nonisothermal catalyst pellet. But, studies on the flows of mass and heat in a porous medium, where the solid matrix subjected to chemical reactions is not a catalyst but a reactant, are very few.

The calcination of limestone is an important gas–solid reaction that was employed extensively in metallurgy and chemical industry [19]. The thermal decomposition of calcium carbonate is a strongly endothermic chemical reaction, forming CO_2 gas. So it is necessary to absorb substantive heat from the environment when the reaction rate is higher, and a macroscopic volume flow of product gas from the reaction interface to the main stream will be induced. As a result, the reciprocal coupling among the heat transfer, mass transfer and the chemical reaction should be investigated, during the calcination of limestone when the temperature gradient and the concentration gradient exist simultaneously.

The objective of this paper is to establish the mathematical model describing the coupled processes of the limestone decomposition reaction, the heat and mass transfer in packed bed, by applying the local thermal non-equilibrium assumption and the Ergun–Forchheimer–Brinkman equation. Differing from the traditional two phase equation model, just the temperature field of bulk flow is known from the solution of energy equation. The temperature distribution of the solid matrix is solved according to the reaction kinetics of the decomposition of calcium carbonate. The coupling of these two equations is given by the item

of chemical reaction. And the model is solved numerically by the alternate dimension implicit method. The profiles of the temperature fields for the fluid and solid phases, the concentration distribution of the product gas and the solid conversion degree are obtained, by changing key parameters. The influence of the strongly endothermic chemical reaction on the heat and mass transfers in the porous medium are discussed.

2. Modeling and formulation

2.1. Problem description

The schematic diagram of the problem is shown in Fig. 1. A cylindrical reactor is filled with spherical specimens and is subject to a constant heat flux boundary condition. The diameter of the circular duct is $2R$, and the length of which is L. Due to symmetry considerations, one half of the reactor is considered.

The following assumptions are invoked in the formulation of the model:

(1) The flow in the porous media is incompressible, i.e. the bulk density of the gas ρ is constant;
(2) The natural convection and the radiation heat transfer are neglected;
(3) The rate of decomposition was controlled by the heat transfer from environment to reactive interface;
(4) The process of heat conductivity through the calcined layer is pseudo-steady state;
(5) The temperature of the unreacted core remained constant;
(6) The entire amount of heat transferred from the environment to the sample was used up for the endothermic reaction and the temperature rise of the product gas diffusion flux.

2.2. Mathematical modeling

According to the shrinking core model, the calcination of limestone is made up of five steps:

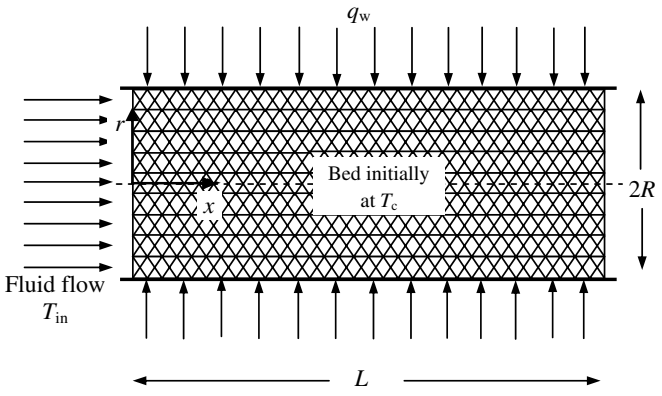

Fig. 1. Schematic diagram of the reactor filled with porous media.

(1) Heat transfer from the environment to the exterior of a particle;
(2) Heat transfer from the particle's external surface to the reaction interface;
(3) At the reaction interface, limestone absorbs heat and begins to decompose thermally;
(4) CO_2 formed by reaction diffuses through a porous layer of CaO, which extends from the reaction interface to the particle's exterior;
(5) The diffusion of CO_2 from a particle's exterior surface to the environment.

The amount of heat that reaches the outer surface of the oxide shell, i.e. the heat transfer rate of step (1), is given by

$$q_s = 4\pi r_{in}^2 h_i (T_b - T_s) \tag{1}$$

The amount of heat that reaches the decomposition interface, i.e. the heat transfer rate of step (2) can be given by the equation [20]

$$q_d = 4\pi \lambda_e r_{in} r_c (T_s - T_c)/(r_{in} - r_c) \tag{2}$$

Because calcination is a relatively slow process, a pseudo-steady state can be assumed [20], so

$$q_s = q_d \tag{3}$$

Substituting Eqs. (1) and (2) in Eq. (3) and solving for T_s

$$T_s = \frac{r_{in} h_i T_b + \lambda_e r_c T_c/(r_{in} - r_c)}{r_{in} h_i + \lambda_e r_c/(r_{in} - r_c)} \tag{4}$$

Substituting Eq. (4) in Eqs .(1) and (2) and rearranging

$$q_s = q_d = \frac{4\pi r_{in}^2 (T_b - T_c)}{[1/h_i + r_{in}(r_{in}/r_c - 1)/\lambda_e]} \tag{5}$$

The heat consumed by chemical reaction (corresponding to step (3)) is given by [20]

$$q_r = R_A\{\Delta H + C_{p,CO_2}(T_b - T_c)\} \tag{6}$$

As we have assumed in part 2.1, the overall rate of decomposition was controlled by the heat transfer from environment to reactive interface. Then the influences of step (4) and step (5) on the overall rate of decomposition can be neglected. These five steps take place in series. The overall rate of the calcination of limestone is determined by the slowest step which is called the control step, and the rates of other steps are all equal to the rate of the slowest step [21]. Thus

$$q_r = q_s = q_d \tag{7}$$

Substituting Eqs. (5) and (6) in Eq. (7) and solving for R_A, then the overall rate formulation in heat transfer controlled regime suitable to single pellet thermal decomposition (R_A) can be obtained as follows

$$R_A = 4\pi r_{in}^2 (T_b - T_c)/\{[1/h_i + r_{in}(r_{in}/r_c - 1)/\lambda_e] \times [\Delta H + C_{p,CO_2}(T_b - T_c)]\} \tag{8}$$

The instantaneous decomposition rate may be given by [20]

$$R_A = -dG_A/dt = -(4\pi r_c^2 \rho_s/M_s)dr_c/dt \quad (9)$$

where $-dG_A/dt$ denotes the exhaustive mole of calcium carbonate per unit volume and unit time. Combining Eqs. (8) and (9), separating the variables and integrating

$$\begin{aligned}(M_s/\rho_s)\int_0^t \{(T_b - T_c)/[\Delta H + C_{p,CO_2}(T_b - T_c)]\}dt \\ = [r_{in}(1-(r_c/r_{in})^3)]/(3h_i) + [r_{in}^2(1-(r_c/r_{in})^2)]/(2\lambda_e) \\ - [r_{in}^2(1-(r_c/r_{in})^3)]/(3\lambda_e)\end{aligned} \quad (10)$$

Defining $X = r_c/r_{in}$, $f_s = 1 - X^3$, f_s is the solid fractional conversion.

Eq. (8) is an overall rate expression, which is only suitable to a single sphere. In packed bed, the minimal unit is the representative elementary volume (REV). In order to derive the overall reaction rate of REV, we need to know the specific surface area of REV which can be written as follows:

$$S_V = 3(1-\varepsilon)/r_{in} \quad (11)$$

From Eqs. (8) and (11), the overall rate formulation R_V can be derived as:

$$\begin{aligned}R_V = [3(1-\varepsilon)/r_{in}](T_b - T_c)/\{[1/h_i + r_{in}(r_{in}/r_c - 1)/\lambda_e] \\ \times [\Delta H + C_{p,CO_2}(T_b - T_c)]\}\end{aligned} \quad (12)$$

The quantity R_V denotes the mole of the product gas CO_2 produced by the decomposition of limestone per unit volume and unit time in packed bed.

The fluid-to-solid heat transfer coefficient is expressed as [6,22]

$$h_i = k_f[2 + 1.1Pr^{1/3}(\rho_f v d/\mu)^{0.6}]/d \quad (13)$$

Considering the diffusion, convection and chemical reaction take place simultaneously in the porous media; the mass balances for product gas CO_2 on the scale of a REV are given by

$$\begin{aligned}\varepsilon\frac{\partial C_{CO_2}}{\partial t} = \varepsilon\frac{1}{r}\frac{\partial}{\partial r}\left(rD\frac{\partial C_{CO_2}}{\partial r}\right) + \varepsilon\frac{\partial}{\partial x}\left(D\frac{\partial C_{CO_2}}{\partial x}\right) \\ - \varepsilon v\frac{\partial C_{CO_2}}{\partial x} + R_V\end{aligned} \quad (14)$$

Substituting Eq. (12) in the above equation

$$\begin{aligned}\varepsilon\frac{\partial C_{CO_2}}{\partial t} = \varepsilon\frac{1}{r}\frac{\partial}{\partial r}\left(rD\frac{\partial C_{CO_2}}{\partial r}\right) + \varepsilon\frac{\partial}{\partial x}\left(D\frac{\partial C_{CO_2}}{\partial x}\right) - \varepsilon v\frac{\partial C_{CO_2}}{\partial x} \\ + \frac{S_v(T_b - T_c)}{\{[1/h_i + r_{in}(r_{in}/r_c - 1)/\lambda_e][\Delta H + C_{p,CO_2}(T_b - T_c)]\}}\end{aligned} \quad (15)$$

v is the effective velocity, the quantity of v can be determined from the superficial velocity v_b and the porosity, $v = v_b/\varepsilon$. The model developed for analyzing the fluid flow in the porous media is the Ergun–Forchheimer–Brinkman equation [23] expressed as follow

$$\begin{aligned}-\frac{dP}{dx} = 150\frac{\mu v_b}{d^2}\frac{(1-\varepsilon)^2}{\varepsilon^3} + 1.75\frac{\rho_f v_b^2}{d}\frac{(1-\varepsilon)}{\varepsilon^3} \\ - \frac{\mu}{\varepsilon}\frac{1}{r}\frac{d}{dr}\left(r\frac{dv_b}{dr}\right)\end{aligned} \quad (16)$$

The energy conservation equation of the main stream is given by

$$\begin{aligned}\varepsilon\frac{\partial(\rho C_p T_b)}{\partial t} = \varepsilon\frac{1}{r}\frac{\partial}{\partial r}\left(rk_f\frac{\partial T_b}{\partial r}\right) + \varepsilon\frac{\partial}{\partial x}\left(k_f\frac{\partial T_b}{\partial x}\right) \\ - \varepsilon v\frac{\partial(\rho C_p T_b)}{\partial x} - S_v\frac{(T_b - T_c)}{\{1/h_i + r_{in}(r_{in}/r_c - 1)/\lambda_e\}}\end{aligned} \quad (17)$$

The surface temperature of the sphere T_s (Eq. (4)) is solved form Eqs. (1) and (2). This formulation is a simplifying approach of the two-temperature model and only suitable to the system with strong endothermic gas–solid reactions.

The following dimensionless variables are introduced for normalizing the governing equations and boundary conditions

$$\begin{aligned}C^* = C_{CO_2}/\rho, \quad \bar{t} = tD/L^2, \quad \bar{r} = r/R, \quad \bar{x} = x/L, \\ T^* = T_b/T_{in}\end{aligned} \quad (18)$$

Utilizing Eq. (18), the dimensionless mass balance equation can be written as:

$$\begin{aligned}\frac{\partial C^*}{\partial \bar{t}} = \frac{L^2}{R^2}\frac{1}{\bar{r}}\frac{\partial}{\partial \bar{r}}\left(\bar{r}\frac{\partial C^*}{\partial \bar{r}}\right) + \frac{\partial^2 C^*}{\partial \bar{x}^2} - \frac{v(\bar{r})L}{D}\frac{\partial C^*}{\partial \bar{x}} \\ + \frac{S_v T_{in} L^2}{\varepsilon\rho D R_1}\frac{(T^* - T_c/T_{in})}{[\Delta H + C_{p,CO_2}T_{in}(T^* - T_c/T_{in})]}\end{aligned} \quad (19)$$

where $R_1 = 1/h_i + r_{in}(r_{in}/r_c - 1)/\lambda_e$.

The specific heat of mixture gas C_p in Eq. (17) can be rewritten as:

$$C_p = (1 - C^*)C_{p,d} + C^* C_{p,CO_2} \quad (20)$$

The dimensionless energy equation is

$$\begin{aligned}\frac{\partial((1-C^*)C_{p,d} + C^* C_{p,CO_2})T^*}{\partial \bar{t}} \\ = \frac{L^2}{R^2}\frac{k_f}{D\rho}\frac{1}{\bar{r}}\frac{\partial}{\partial \bar{r}}\left(\bar{r}\frac{\partial T^*}{\partial \bar{r}}\right) + \frac{k_f}{D\rho}\frac{\partial^2 T^*}{\partial \bar{x}^2} \\ - \frac{v(\bar{r})L}{D}\frac{\partial((1-C^*)C_{p,d} + C^* C_{p,CO_2})T^*}{\partial \bar{x}} \\ - \frac{S_v L^2}{D\rho}\frac{(T^* - T_c/T_{in})}{\{1/h_i + r_{in}(r_{in}/r_c - 1)/\lambda_e\}}\end{aligned} \quad (21)$$

3. Numerical solution

Alternate dimension implicit method (ADI) [24,25] was used to solve the two-dimensional mathematical model established in this paper numerically. The ADI formulation can be constructed by discretizing the partial differential governing equations and then splitting the space as alternatively let each spatial direction be represented implicitly while the other explicitly at 1/2 time

interval. In this way, a two-dimensional problem was transformed into two series-wound one-dimensional implicit problems. The initial and boundary conditions for the problem are: $C^*(\bar{x},\bar{r},0)=0$, $T^*(\bar{x},\bar{r},0)=T_c/T_{in}$, $r_c(\bar{x},\bar{r},0)=r_{in}$, $C^*(0,\bar{r},\bar{t})=0$, $T^*(0,\bar{r},\bar{t})=1$, $\partial C^*(\bar{x},0,\bar{t})/\partial\bar{r}=0$, $\partial T^*(\bar{x},0,\bar{t})/\partial\bar{r}=0$, $\partial C^*(1,\bar{r},\bar{t})/\partial\bar{x}=0$, $\partial T^*(1,\bar{r},\bar{t})/\partial\bar{x}=0$, $\partial C^*(\bar{x},1,\bar{t})/\partial\bar{r}=0$, $\partial T^*(\bar{x},1,\bar{t})/\partial\bar{r}=q_w$.

The discrete equations can not be solved independently because of the cross-coupling between the mass balance equation and the energy balance equation, so an iterative method was used to solve the temperature and concentration fields. Convergence is measured in terms of the maximum change in each variable during iteration at each time increment. The maximum change allowed for the convergence check is set to 10^{-6}. All computations have been carried out for a half of the cylindrical reactor $L\times R$ using non-uniform grid arrangements with 60×50 to ensure that the results are independent of the grid system.

4. Results and discussion

The values of the constant parameters in calculation are given by: $C_{p,d}=27.972$ J mol^{-1} K^{-1}, $C_{p,\ CO2}=44.31$ J mol^{-1} K^{-1}, $k_f=0.072$ W m^{-1} K^{-1}, $D=3.05\times10^{-4}$ m^2 s^{-1}, $\rho_s=2.47\times10^3$ Kg m^{-3}, $L=0.15$ m, $R=0.05$ m, $T_c=1170$ K, $\lambda_e=0.0053$ W m^{-1} K^{-1}, $\Delta H=161.91$ KJ mol^{-1} [20].

In order to verify the present theoretical model, a simulation of the experimental conditions of literature [19] was performed. The numerical solutions of the present model for the conversion ratio were compared with the experimental data as shown in Fig. 2. The dotted lines in Fig. 2 show the experimental data for the variation of the conversion ratio with time for three different particle sizes, and the calculated results are represented by the solid lines. An excellent agreement can be seen between the measurements and calculations.

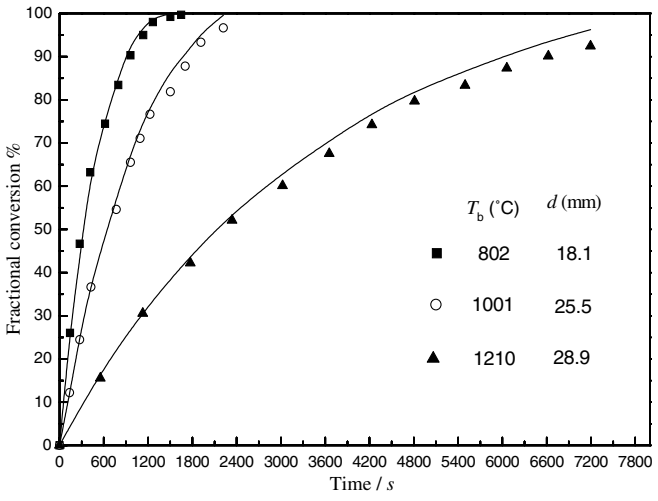

Fig. 2. Comparison of the calculated curves with the experimental data in literature [19] ($T_c=800$ °C, $\varepsilon=0.09$).

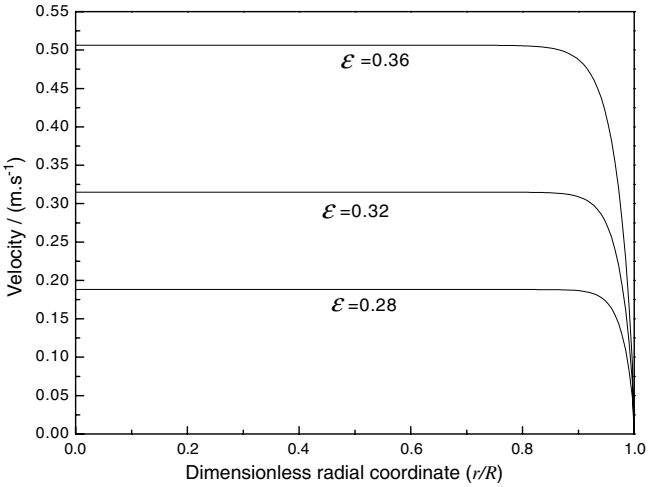

Fig. 3. Variation of velocity profile with porosity ($t=330$ s, $T_{in}=1100$ °C, $r_{in}=2$ cm).

The penetrative velocity profiles in the radial direction obtained by using the Ergun–Forchheimer–Brinkman equation are shown in Fig. 3. demonstrates that as the porosity increases, the penetrative velocity increases significantly. The penetrative velocity decreases obviously at the radial boundary wall and a velocity boundary layer is formed. The third term on the right-hand side of Eq. (16) is the Brinkman term, which represents the viscous effects introduced by the presence of an interface region and ensures the no-slip boundary condition at the wall. Although the momentum boundary layer is in general confined to a small distance from the wall, its inclusion in the analysis is crucial for computing the distributions of temperature and concentration in the undergoing investigation.

The influences of the penetrative velocity of the bulk flow on the transport and reaction characteristics along the axial centerline of the porous reactor are shown in Figs. 4–6. It can be seen from Fig. 4 that the larger the convection rate is, the more significant the temperature difference between the fluid and solid phases is. In addition, increasing the penetrative velocity of the feeding gas leads to the conversion degree of the solid particles enhances while the concentration distribution of the product gas reduces, as shown in Figs. 5 and 6. This is expected since a higher flow rate would cause more heat to be transferred into the reactor and more product gas to be transferred outward from the reactor, which results in the increase in the reaction rate and the decrease in the concentration of product gas.

Fig. 7 shows the variation of the fluid and solid temperature fields, the concentration distribution of the product gas and the conversion ratio of the solid particles with the initial temperature of feeding gas in radial direction of the porous packed bed. As can be seen from Fig. 7a, the temperature fields for both phases increase as T_{in} increases and the temperature differences between the two phases enhance at the same time. The results imply that

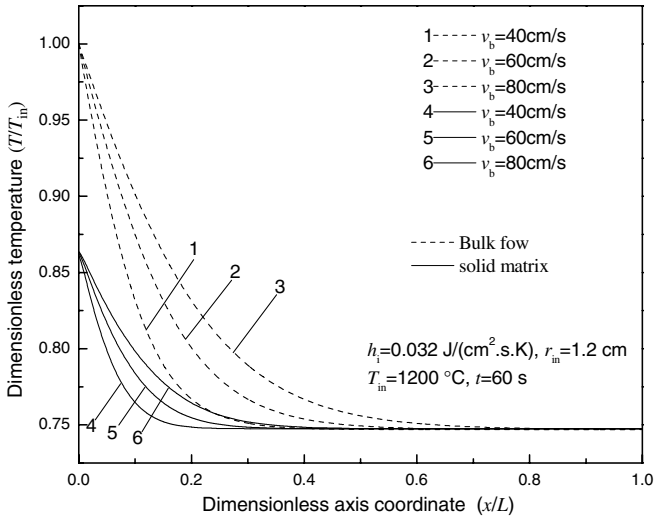

Fig. 4. Effect of convectional velocity on the temperature fields for gas and solid matrix.

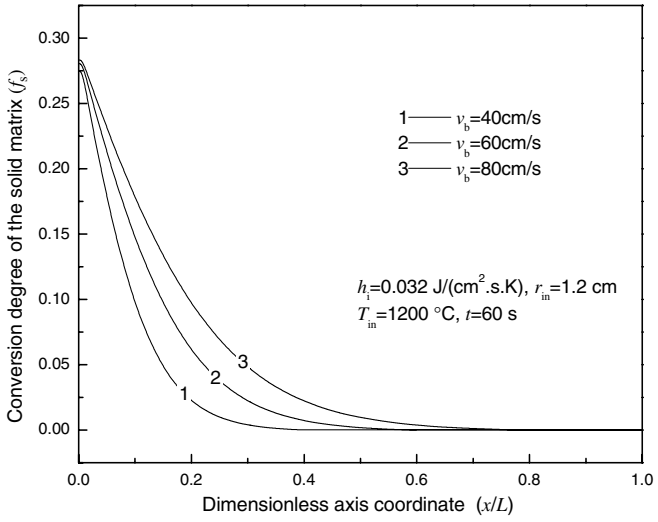

Fig. 5. Variation of the fractional conversion of solid matrix with convectional velocity.

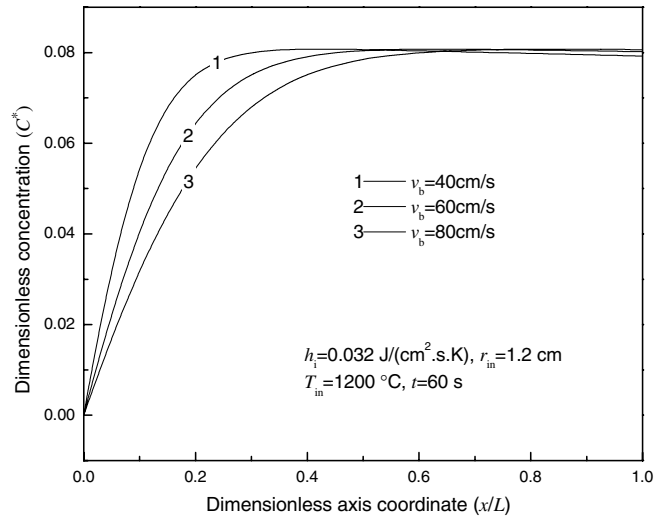

Fig. 6. Effect of convectional velocity on the concentration fields of the product gas.

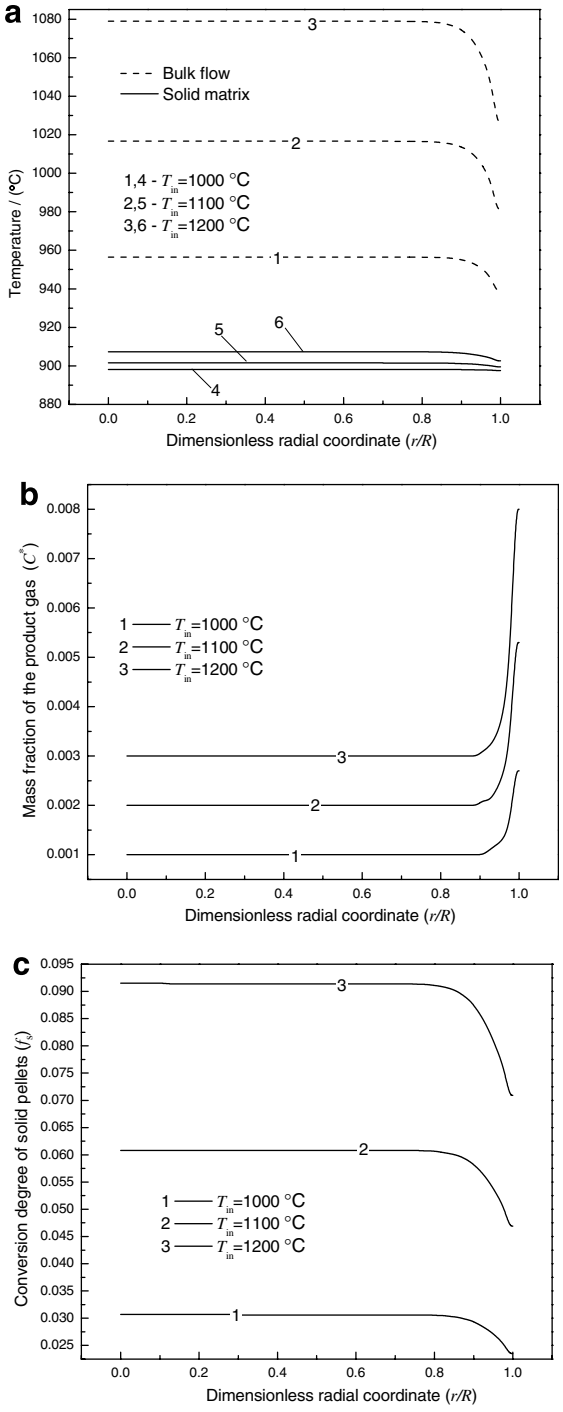

Fig. 7. Variation of various quantities in different initial temperature of feeding gas at the cross section of $x = 0.0024$ m. ($t = 90$ s, $v_b = 37.79$ cm/s, $r_{in} = 1$ cm, $\varepsilon = 0.32$): (a) Radial temperature fields of the bulk flow and the solid matrix. (b) Concentration distribution of the product gas. (c) Conversion degree of solid pellets.

increasing the initial temperature of feeding gas would cause a higher departure from the local thermal equilibrium condition. It was also found that the product gas concentration distribution and the conversion ratio of the solid particles all increase with the increase of the initial temperature (Fig. 7b and c). This is expected since a higher initial temperature of feeding gas would cause the quantity of

heat transferred into the reactor to improve, which results in the increase in the decomposition reaction rate. Consequently, the solid reactant consumed by thermal decomposition reaction increases, and more product gas is produced. It is worth pointing out that the profiles of the temperature distributions of the two phases and the solid conversion ratio all decay near the radial boundary wall $\bar{r} = 1$, which corresponding to the boundary layer of the velocity in Fig. 3. However, the concentration of the product gas increases near the wall owing to the slower speed layer.

Figs. 8–10 display the effect of the particle diameter on the gas and solid temperature fields as well as the chemical characteristics of the porous packed bed. It can be seen from Fig. 8, a larger temperature discrepancy between the fluid and the solid phases was encountered as particle diameter increases. According to Eq. (11), the specific surface area S_V reduces with the increase of the particle diameter, causing the thermal decomposition reaction rate to decrease. Thus, within the same time, if the particle diameter increases, the heat exhausted by the reaction will decrease and the gas produced by reaction also reduced (Fig. 9). Fig. 10 exemplifies the effect of the particle diameter on the solid conversion degree. As can be concluded from this figure, the solid conversion degree reduces near the entrance as the particle radius increases. But with the region that takes place the decomposition reaction deepens down to the exit, an increase in particle diameter results in an opposite effect for the solid conversion degree. This is expected since the overall reaction rate (Eq. (12)) is determined by the product of the specific surface area S_V and the temperature difference between the two phases $(T_b - T_c)$. Hence, the variation of the solid conversion degree with particle diameter is diverse at different spatial coordinate.

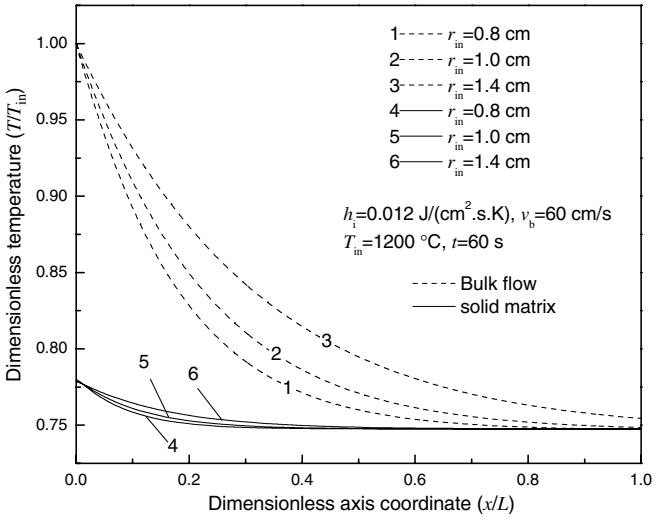

Fig. 8. Influence of the particle radius on the temperature field of the gas and solid matrix.

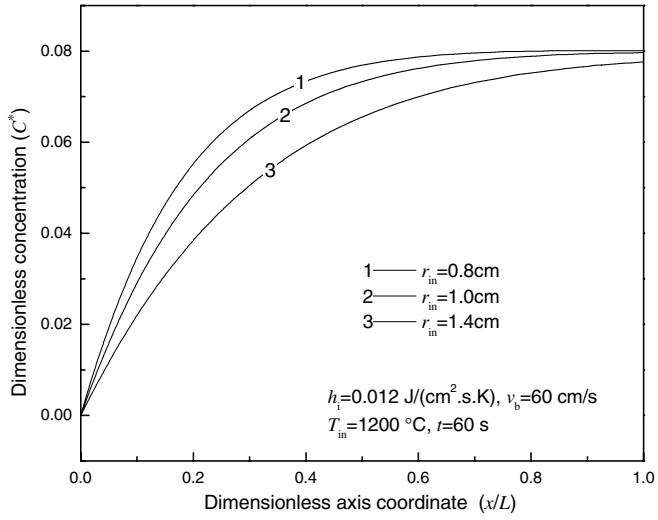

Fig. 9. Variation of the concentration fields of the product gas with the particle radius.

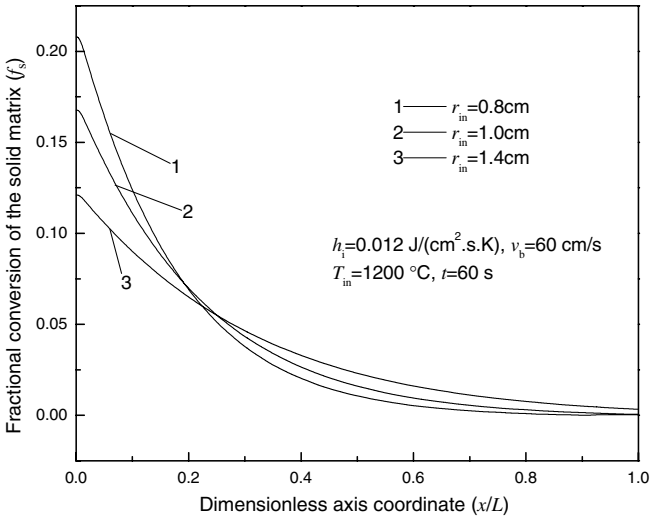

Fig. 10. Influence of the particle radius on the fractional conversion of solid matrix.

5. Conclusion

According to the chemical reaction kinetics and the assumption of local thermal non-equilibrium, a mathematical model describing the coupling among the multi-irreversible processes in a porous system with a strong endothermic chemical reaction was established and solved by the alternate dimension implicit method. The calculated results showed that, the temperatures difference between the fluid and solid phases can not be ignored during the study of limestone calcination. The temperature fields for both phases and the temperature differences between the two phases all enhance, resulting from the increase either in the penetrative velocity or in the initial temperature of feeding gas or in the particle diameter. Corresponding to the boundary layer of the velocity, the profiles of the temperature distributions of the two phases and the solid conversion ratio all decay near the radial boundary wall

$\bar{r} = 1$. However, the concentration of the product gas increases near the wall owing to the slower speed layer. The concentration distribution of the product gas reduced as the penetrative velocity quickens, but increased with the increase of the initial temperature T_{in}. Depending on the specific value of the overall reaction rate, the variation of the solid conversion degree with particle diameter is diverse at different spatial coordinate. This will be useful for the design of reactor and choosing the most reasonable operation conditions.

References

[1] P. Cheng, Heat transfer in geothermal systems, Adv. Heat Transfer 14 (1978) 1–105.

[2] D.A.S. Rees, K. Vafai, Darcy–Brinkman free convection from a heated horizontal surface, Numer. Heat Transfer A: Appl. 35 (1999) 191–204.

[3] S.J. Kim, K. Vafai, Analysis of natural convection about a vertical plate embedded in a porous medium, Int. J. Heat Mass Transfer 32 (1989) 665–677.

[4] S. Whitaker, Local thermal equilibrium: an application to packed bed catalytic reactor design, Chem. Eng. Sci. 41 (1986) 2029–2039.

[5] M. Quintard, S. Whitaker, One- and two-equation models for transient diffusion processes in two-phase systems, Adv. Heat Transfer 23 (1993) 369–464.

[6] A. Amiri, K. Vafai, Transient analysis of incompressible flow through a packed bed, Int. J. Heat Mass Transfer 41 (1998) 4259–4279.

[7] S.J. Kim, D. Kim, D.Y. Lee, On the local thermal equilibrium in microchannel heats sinks, Int. J. Heat Mass Transfer 43 (2000) 1735–1748.

[8] E.U. Schlunder, Equivalence of One- and two-phase models for heat transfer processes in packed beds: one-dimensional theory, Chem. Eng. Sci. 30 (1975) 449–452.

[9] M. Quintard, Modelling local non-equilibrium heat transfer in porous media, Proceedings of the 11th International Heat Transfer Conference 1 (1998) 279–285.

[10] D.Y. Lee, K. Vafai, Analytical characterization and conceptual assessment of solid and fluid temperature differentials in porous media, Int. J. Heat Mass Transfer 42 (1999) 423–435.

[11] A.V. Kuznetsov, Thermal non-equilibrium, Non-Darcian forced convection in a channel filled with a fluid saturated porous medium – a perturbation solution, Appl. Sci. Res. 57 (1997) 119–131.

[12] A. Marafie, K. Vafai, Analysis of non-Darcian effects on temperature differentials in porous media, Int. J. Heat Mass Transfer 44 (2001) 4401–4411.

[13] K. Vafai, M. Sozen, Analysis of energy and momentum transport for liquid flow through a porous bed, J. Heat Transfer Trans. ASME 112 (1990) 690–699.

[14] M. Quintard, S. Whitaker, Two-phase flow in heterogeneous porous media I. The influence of large spatial and temporal gradients, Trans. Porous Media 5 (1990) 341–379.

[15] D.Y. Lee, K. Vafai, Comparative analysis of jet impingement and microchannel cooling for high heat flux applications, Int. J. Heat Mass Transfer 42 (1999) 1555–1568.

[16] B. Alazmi, K. Vafai, Constant wall heat flux boundary conditions in porous media under local thermal non-equilibrium conditions, Int. J. Heat Mass Transfer 45 (2002) 3071–3087.

[17] J.W. Veldsink, R.M.J. van Damme, G.F. Versteeg, W.P.M. van Swaaij, The use of the dusty-gas model for the description of mass transport with chemical reaction in porous media, Chem. Eng. J. 57 (1995) 115–125.

[18] D.N. Jaguste, S.K. Bhatia, Simulation of reaction and transport in catalyst particles with partial external and internal wetting, Int. J. Heat Mass Transfer 38 (1995) 1443–1455.

[19] E.T. Turkdogan, R.G. Olsson, H.A. Wriedt, L.S. Darken, Calcination of limestone, Trans. Soc. Min. Eng. AIME 254 (1973) 9–21.

[20] G. Narsimhan, Thermal decomposition of calcium carbonate, Chem. Eng. Sci. 16 (1961) 7–20.

[21] M. Iwao, T. Junichiro, M. Akira, Reaction kinetics in the blast furnace, J. Jpn. Inst. Metals 30 (1966) 826–831.

[22] A. Amiri, K. Vafai, T.M. Kuzay, Effects of boundary conditions on non-Darcian heat transfer through posous media and experimental comparisons, Numer. Heat Trans. A 27 (1995) 651–664.

[23] M. Sozen, T.M. Kuzay, Enhanced heat transfer in round tubes with porous inserts, Int. J. Heat Fluid Flow 17 (1996) 124–129.

[24] W.F. Ames, Numerical Methods for Partial Differential Equations, Academic Press, New York, 1977.

[25] W.Q. Tao, E.M. Sparrow, Transportive property and convective numerical stability of the steady-state convective-difference equation, Numer. Heat Trans. 11 (1987) 491–497.